ARTICLE

Magnetic Particles used in a New Approach for Designed Protein Crystallization

Received 00th January 20xx,
Accepted 00th January 20xx

DOI: 10.1039/x0xx00000x

Raquel dos Santos[a], Maria João Romão[a], Ana Cecília Roque[a]*, and Ana Luísa Carvalho[a]*

After more than one hundred and thirty thousand protein structures determined by X-ray crystallography, the challenge of protein crystallization for 3D structure determination remains. In the quest for additives for efficient protein crystallization, inorganic materials emerge as an alternative. Magnetic particles (MPs) are versatile inorganic materials, easy to use, modify and manipulate in a wide range of biological assays. The potential of using functionalised MPs as crystallization chaperones for protein crystallization was shown in this work. MPs with distinct coatings were rationally designed to promote protein crystallization by affinity-triggered heterogeneous nucleation. Hen egg white lysozyme (HEWL) and trypsin, were crystallized in the presence of MPs either bare or coated with a polysaccharide (chitin) or a protein (casein), respectively. The addition of MPs was characterized in terms of bound protein to the MPs, crystal morphology, time-lapse of crystal emergence, crystallization yield fold change and crystal diffraction quality for structure determination. The MPs additives have shown to bind to the respective target protein, and to promote nucleation and crystal growth without compromising crystal morphology. On the other hand, MPs addition led to faster detectable crystal emergence and up to 13 times higher crystallization yield, addressing some the challenges in protein crystallization, the main bottleneck of macromolecular crystallography. Structure determination of the protein crystallized in the presence of MPs revealed that the structural characteristics of the protein remained unchanged, as shown by the superposition with PDB annotated proteins. Moreover, and unlike most reported cases, it was possible to exclude the inhibitor benzamidine during trypsin crystallisation, which is a remarkable result opening new prospects in enzyme engineering and drug design. Our results show that MPs coated with affinity ligands to target proteins can be used as controlled and tailor-made crystallization inducers.

Introduction

High-resolution structure determination of macromolecules, alone or in complex with ligands, is a powerful tool in protein engineering and drug design. Protein structural information is one of the key steps to control or improve its function, by rationally designing small binding molecules [1] (e.g. agonist or antagonist drugs), or by engineering mutants with a desirable biological activity [2]. On the other hand, the three-dimensional high-resolution structure of molecular complexes can unveil macromolecule-ligand interactions enhancing its biotechnological applications in fields such as biocatalysis [3], sensing material development [4], macromolecule function redesign [5], or in the downstream processing field [6].

One of the most powerful tools for high-resolution structure determination is X-ray crystallography, providing a 3D structure with atomic resolution of a single protein, protein-DNA complex, protein-protein or a protein-ligand complex. X-ray crystallography requires high-quality protein crystals for X-ray diffraction. However, the major bottleneck still lies in finding the conditions that give rise to diffraction-quality single crystals, added to reliable reproducibility. This can be overcome by developing new and more efficient crystallization screening protocols, but also by introducing new additives that can act as nucleation agents for protein crystal growth. These additive compounds, also designated as nucleants, promote heterogeneous nucleation, often occurring on a surface in contact with the protein/precipitant solution [7]. Most commonly, although poorly understood, impurities can promote nucleation.

Protein crystallization occurs under saturated conditions, by changing the protein environment until exceeding the protein solubility limit, leading to nucleation and crystal growth. The supersaturation environment is often empirically determined. Although classical nucleation theory and phase diagram plots may enlighten the interactions promoting protein crystallization, the fact is that protein crystallization is still an empirical process. The formation of a protein crystal starts with the nucleation phase in which the protein molecules, in the supersaturated solution, become arranged in a specific repetitive pattern, characteristic of the crystalline form. Then, additional protein molecules are deposited on the nucleus surface and the crystal grows in progressive layers. To overcome some of the protein crystallization challenges (onset of nucleation, reduce solvent content or prepare heavy atom

[a] UCIBIO, Chemistry Department, School of Science and Technology, NOVA University of Lisbon, 2829-516 Caparica, Portugal
* Corresponding Authors: cecilia.roque@fct.unl.pt; almc@fct.unl.pt
† Electronic Supplementary Information (ESI) available: [details of any supplementary information available should be included here]. See DOI: 10.1039/x0xx00000x

derivatives), new additives with nucleation properties are frequently tested [8,9]. Traditional additives commonly found in the crystallization screening protocols rely mainly on surfactants, organic compounds (e.g. 2-propanol, 1,4-dioxane or glycerol), mono- and multivalent salts, reducing agents (e.g. dithiothreitol, 2-mercaptoethanol and tris(2-carboxyethyl)phosphine (TCEP)), amino acids or monosaccharides. New additives can be of biological source, such as DNA origami [10] and cyclic oligosaccharides [11], or of non-biological origin as small synthetic ligands [9] or nanoscale materials [12]. In particular, new nanoscale materials, namely nanoparticles made of gold, porous silicon or nanodiamonds, as well as carbon nanotubes, have already been successfully used as nucleation agents to trigger crystal growth in different protein crystallization studies for 3D structure determination [13–17].

Magnetic particles with an iron oxide (Fe_3O_4) core, typically with core-shell structures, are another class of nanomaterials used in the context of protein crystallization. Among the advantages of magnetic particles, they are low cost, easy to produce and handle, and able to be tailored with different coatings and functionalization. In addition, and due to their superparamagnetic core, these particles can be easily separated from a solution by applying an external magnetic field and have the potential to be reversibly resuspended back in solution in magnetic fishing separation [18–20].

Here, we studied the potential of using magnetic particles as additives in protein crystallization. Two proteins were selected as model case studies: hen egg white lysozyme (HEWL) and bovine pancreatic trypsin. To promote the selective binding of the target protein to the surface of the magnetic particles, known affinity ligands for HEWL and trypsin were coated to the surface of the particles. Each affinity ligand was selected based on previous knowledge about its interaction with the target protein. Chitin was the polysaccharide of choice to bind HEWL [21], and casein was selected as the biological ligand for trypsin [22]. The obtained protein single crystals were further evaluated in terms of X-ray diffraction quality. Our results indicate that the presence of magnetic particles as crystallization additives did not significantly affect the maximum resolution limits or unit cell parameters, maintaining crystal isomorphism when compared to native conditions. Furthermore, the addition of magnetic particles led to the increase of crystallization yield and remarkably enabled the reproducible crystallization of trypsin in the absence of its inhibitor benzamidine, often required in trypsin crystallization assays.

Results and discussion

The effect of magnetic particles as additives in crystallization

Magnetic particles (MPs) were produced and chemically modified with affinity ligands tailoring each of the target proteins, namely MP-chitin for hen egg white lysozyme (HEWL) and MP-casein for trypsin. In brief, MPs were characterized by Fourier-transform infrared spectroscopy (FT-IR), transmission electron microscopy (TEM), dynamic light scattering (DLS) and zeta potential (Fig. S1 and Table S1, †ESI). Particles with a spherical shape and 5 - 10 nm in diameter (confirmed by TEM) were successfully functionalized (confirmed by FT-IR spectra; Figure S1A-B, †ESI). DLS and zeta potential analyses were performed both in water and in the crystallization conditions for each target proteins. Overall, bare MPs (MP-Fe_3O_4) present a smaller hydrodynamic diameter when compared with the functionalized MPs in water and in the respective crystallization conditions. Regarding the zeta potential, MP-Fe_3O_4 and functionalized MPs present the same range of stability in water and in the respective crystallization conditions (Table S1, †ESI). Crystal growth and crystallization yield (yield fold change) were assessed using MP-Fe_3O_4 as nucleation agent for HEWL crystallization. Crystal size measurement was impaired by the opacity of MPs in the crystallization drop, hence this was not a reliable method to assess the influence of MPs in protein crystal growth (Fig. 1A). Nonetheless, having MP-Fe_3O_4 as additives enhanced HEWL crystal growth in all concentrations tested, from 0.5 mg/ml up to 4 mg/ml of MPs. The yield fold change, always having as threshold the HEWL crystallization in the absence of MPs, demonstrated the positive effect (crystal yield >1) of MPs as additives by enhancing the mass of protein crystallized per assay (Fig. 1B). The data suggested an association between the concentration of MPs added and an increase in protein crystallized. An increase from 1.5 to 1.9 in yield fold change was observed in the presence of 0.5 and 4 g/l of MP-Fe_3O_4, respectively. Since the increase of crystal growth was not proportional to the increase in MP concentration, for subsequent assays, 0.5 mg/ml of MPs were used as standard MPs concentration to facilitate observations at the microscope. The effect of the addition of MP-Fe_3O_4 (0.5 mg/ml) was also assessed in the crystallization of trypsin. These additives had a notorious effect in the amount of trypsin crystallized, as seen in the major difference in amount of protein crystallized in the presence and absence of MP-Fe_3O_4 (Fig. 1C), with up to 12 times more protein crystallized in the presence of MP-casein.

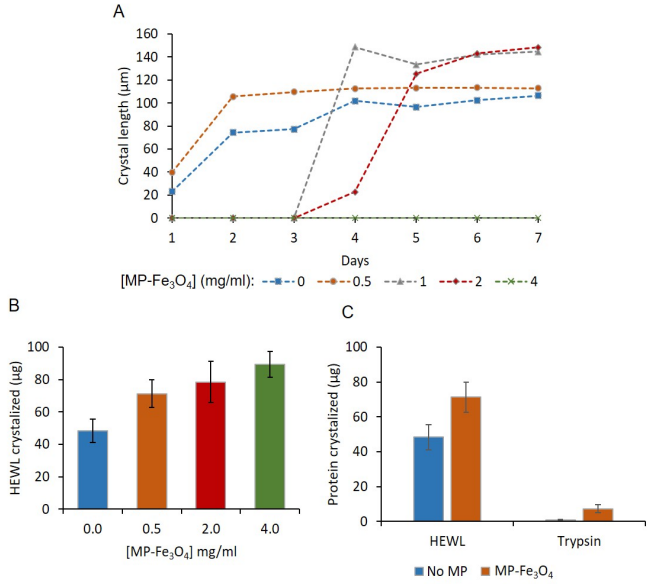

Figure 1. Effect of MPs in protein crystal growth (n=3). (A) Average crystal longest length of visual measurement of HEWL crystals over 7 days in the presence of MP-Fe_3O_4 at different concentrations: 0 mg/ml (■); 0.5 mg/ml (●); 1 mg/ml (▲); 2 mg/ml (♦) and 4 mg/ml (X). (B) HEWL (25 mg/ml) amount of protein crystallized in the presence of MP-Fe_3O_4 at different concentrations (0, 0.5, 2.0 and 4.0 mg/ml). (C) HEWL (25 mg/ml) and trypsin (60 mg/ml) crystallization yield fold change between crystals grown in the presence of no MP and 0.5 mg/ml of MP-Fe_3O_4.

The effect of affinity-triggered magnetic crystallization

As HEWL binds to chitin [21], iron oxide MPs coated with chitin (MP-chitin) were evaluated in terms of binding capacity under the HEWL crystallization conditions (Table 1). The binding assay of HEWL at 25 mg/ml to both particles - MP-Fe_3O_4 and MP-chitin - at 0.5 mg/ml showed yields higher than 50% (>12.5 g HEWL/g support, Table 1). The static binding capacity data of both isotherms were fitted to the Hill plot, since it was the best model to fit the MP-chitin/HEWL binding, to assess the binding parameters for HEWL to both MP-Fe_3O_4 and MP-chitin. The summarized data is shown in Table S2 (†ESI). The static binding capacity data (Table 1 and Table S2, †ESI) suggested that HEWL binds to both MP-Fe_3O_4 and MP-chitin at static conditions, as indicated by the Q_{max} calculated, K_a and Hill coefficient.

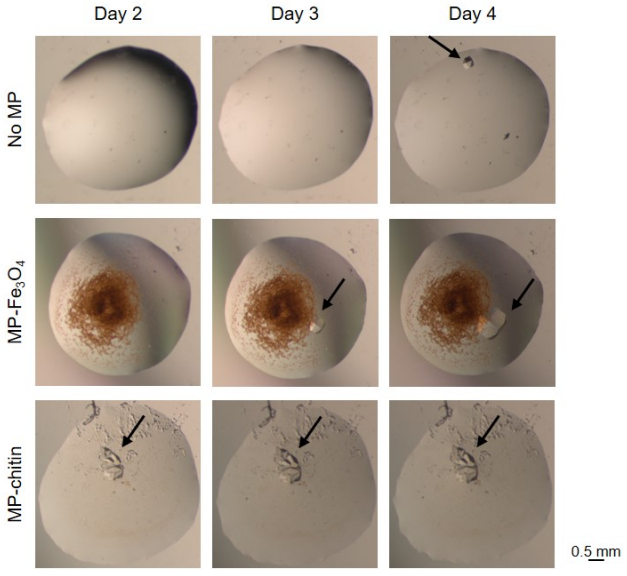

Figure 2. HEWL (25 mg/ml) crystallization in the absence and presence of MP-Fe_3O_4 and MP-chitin (0.5 mg/ml). Visual inspection of days 2, 3 and 4 of crystal growth. Black arrows indicate protein crystal.

Table 1. HEWL adsorption to MP-Fe_3O_4 and MP-chitin (n=3) and trypsin adsorption to MP-Fe_3O_4 and MP-casein in the presence and absence of benzamidine. Binding of 25 mg/ml HEWL in 50 mM CH_3COONa at pH 4.5 to 0.5 mg/ml of MP-Fe_3O_4 and MP-chitin in 0.5 M NaCl (n=3). Binding of 60 mg/ml trypsin in 3 mM $CaCl_2$ in the presence and absence of benzamidine in the protein solution to 0.5 mg/ml of MP-Fe_3O_4 and MP-casein in 0.2 M $(NH_4)_2SO_4$, 30% (w/v) PEG8000.

	Bound protein (g protein/g support)	
	MP-Fe_3O_4	**MP-affinity**
HEWL	17.8 ± 0.7	22.4 ± 1.1
Trypsin (without benzamidine)	206.4 ± 1.7	206.88 ± 2.2
Trypsin (with benzamidine)	127.7 ± 0.5	126.4 ± 2.9

A crystallization period of 4 days [13,16,23] was recorded to assess if the magnetic (MP-Fe_3O_4) and affinity-triggered magnetic (MP-chitin) crystallization had an effect in crystal growth (nucleation time and maximum dimensions). As an example, Fig. 2 shows the time course of crystal growth for 3 drops with no MPs, MP-Fe_3O_4 and MP-chitin. The affinity-triggered magnetic crystallization led to an earlier visible onset of HEWL crystals by day 2. The presence of MP-Fe_3O_4 did not cause such fast-triggering effect in crystal nucleation as MP-chitin, but still HEWL crystals appeared at day 3, one day earlier than under the crystallization conditions without MPs. The condition with no MPs, not only led to a delayed crystal visible onset, but at the same time, by day 4 the crystal was 3 times smaller than in the presence of MPs (Fig. 2). This suggests that the non-specific and random binding of proteins to the bare iron oxide surface, does not trigger as efficiently crystal nucleation and growth, when compared to the specific and oriented binding of proteins to the affinity-functionalized MPs.

Prior work demonstrated the feasibility of purifying trypsin from a complex mixture by magnetic fishing with iron oxide core MPs coated with casein [22]. The binding capacity of trypsin to MP-Fe_3O_4 and MP-casein was calculated in trypsin's crystallization conditions, and binding results were best fitted by the Hill equation (Table 2 and Table S2, †ESI). Overall, the MP-casein performed better for trypsin binding than MP-Fe_3O_4 in terms of K_a and Q_{max}. Once again, the addition of MPs has a notorious effect in the amount of protein crystallized, as seen in the major difference in yield fold change in the presence and absence of MPs (Fig. 3A), with up to 13 times more protein crystallized in the presence of MP-casein. The increment of crystal growth was confirmed by visual inspection (Fig. 3B).

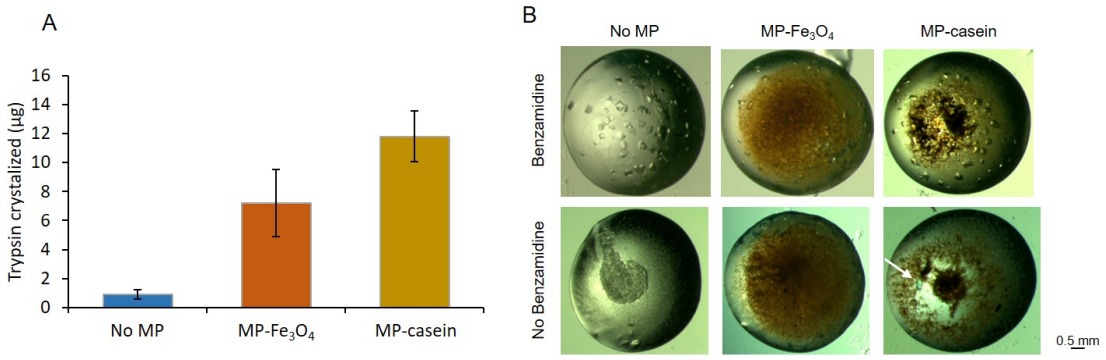

Figure 3. Trypsin adsorption to MP-Fe_3O_4 and MP-casein (n=3). (**A**) Trypsin (60 mg/ml) amount of protein crystallized in the presence of no MP; MP-Fe_3O_4 and MP-casein. (**B**) Trypsin (60 mg/ml) crystallization in the absence and presence of MP-Fe_3O_4 and MP-casein (0.5 mg/ml) in the with and without benzamidine (10 mg/ml) present in the protein solution. Visual inspection was performed at day 30 of crystal growth. White arrow indicates protein crystal.

Magnetic crystallization for proteases

Trypsin, being a protease, is many times crystallized in the presence of benzamidine, a competitive inhibitor of trypsin, trypsin-like enzymes and serine proteases [24–26]. In this work, the presence of benzamidine in the crystallization conditions was assessed in terms of trypsin's binding capacity to both MPs - MP-Fe_3O_4 and MP-casein. Casein was chosen as an affinity-triggered biological ligand for trypsin crystallization as it was reported to be a nonspecific substrate of the proteases [22].

The binding capacity of trypsin to MP-Fe_3O_4 and MP-casein was determined in trypsin's crystallization conditions – in the presence and absence of benzamidine (Table 1 and Table S2, †ESI). The presence of benzamidine impaired trypsin binding to both MPs (Table 1), as it was corroborated by the static binding capacity results (Table S2, †ESI). This could be due to benzamidine occupying trypsin's binding site to the MPs or by benzamidine binding to the MPs. The presence of benzamidine led to lower K_a and Q_{max}, whereas the absence of benzamidine led to higher K_a, up to one order of magnitude higher (Table S2, †ESI). The higher K_a and Q_{max} observed in the absence of benzamidine raises the hypothesis that either benzamidine and casein bind to the same trypsin residues, hampering casein to bind trypsin, or some conformational change in trypsin occurs when bound to benzamidine, impeding casein to bind. Overall, the MP-casein performed better for trypsin binding than MP-Fe_3O_4 in terms of K_a and Q_{max}, (Table S2, †ESI). Once established the effect of benzamidine in MPs binding, the effects in trypsin crystallization in the absence of MPs, presence of MP-Fe_3O_4 and MP-casein, with and without the addition of benzamidine, were

assessed (Fig. 3B). The presence of benzamidine led to higher nucleation rate and crystal size. In contrast, the lack of benzamidine in the crystallization drop led to protein precipitation and therefore, no crystal appearance in the drops without MPs and with MP-Fe_3O_4 (Fig. 3B). When no inhibitor was added, the only condition in which it was possible to achieve protein crystallization was in the presence of MP-casein. The affinity-triggered crystallization led to crystal growth in conditions that otherwise would result in protein precipitation. Crystal growth was observed in 2 out of 3 crystallization drops in which MP-casein were added, while excluding the inhibitor.

X-ray diffraction studies

To assess diffraction quality and isomorphism of the crystals obtained in the presence of MPs, in comparison to reported crystallization conditions for HEWL and trypsin, X-ray diffraction studies were performed to completion.

Primary evaluation of the effect of MPs in crystal morphology was done by comparative analysis of the indexed space groups and cell parameters for the crystals of each protein. In the presence of the correspondent MPs, trypsin crystals kept the original $P2_12_12_1$ space group, and the same happened with HEWL, which crystallized in space group $P4_32_12$, as originally reported (Table 2). Unit cell parameters for HEWL in the presence of MPs were a=b=79.0 Å, c=37.0 Å and α=β=γ=90.0°. Unit cell parameters for bovine trypsin in the presence of MPs were a=54.2 Å, b=58.2 Å, c=66.3 Å and α=β=γ=90.0°. All unit cell parameters are within values comparable with the reference structures [27] (Table 2). After structure solution and refinement, the 3D structures were superposed (in PyMol, Cealign) with PDB available structures from crystals grown in similar precipitant conditions, but in the absence of the additives under study HEWL crystals grown in the presence of MP-chitin were superimposed to HEWL PDB ID: 6F1L [28], presenting an 0.5 Å root mean square deviation (r.m.s.d.) for 120 Cα atoms (Fig. 4A). The 3D structure of trypsin obtained from a crystal grown in the presence of MP-casein and benzamidine was superposed with PDB ID: 5MNG [27], presenting an 0.26 Å r.m.s.d. for 216 Cα atoms (Fig. 4B).

The X-ray crystallography results in this study show that magnetic particles can behave as nucleating agents without changing crystal morphology or protein structure. This is in accordance with previous studies on crystallization additives [12].

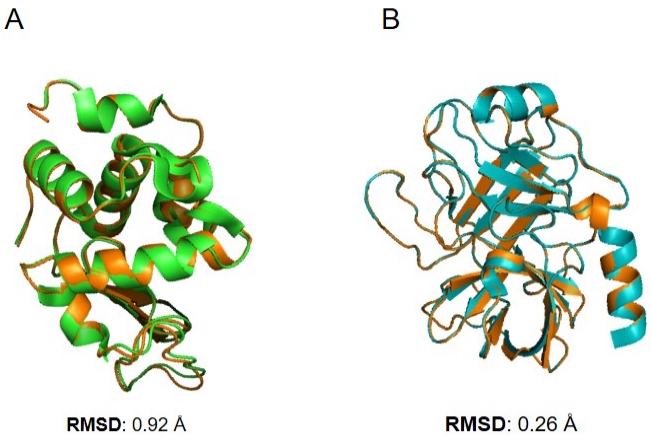

Figure 4. Superposition of the 3D structures obtained from crystals grown in the presence of MPs with corresponding representative structures available in the PDB (rmsd values were calculated in PyMol Cealign). (**A**) HEWL 3D structure from a crystal grown in the presence of MP-chitin and HEWL from PDB ID: 6F1L, presenting a rmsd. of 0.92 Å for the matching of 120 Cα atoms. (**B**) Trypsin 3D structure from a crystal grown in presence of MP-casein and trypsin from PDB ID: 5MNG, presenting a rmsd. of 0.26 Å for the matching of 126 Cα atoms.

Table 2. Affinity-triggered magnetic crystallization conditions. Proteins reported crystallization conditions and respective space group and unit cell parameters obtained by X-ray diffraction [27](to be published, for HEWL), and the affinity ligands used in the development of the affinity-triggered magnetic crystallization assay.

Reference protein structure (PDB Code)	Molecular weight	Reported crystallization conditions	Space group	Unit cell parameters (Å)	Affinity ligand
HEWL (PDB 6QWY)	14.4 kDa	Protein solution: 50 mM CH_3COONa at pH 4.5 Precipitant solution: 0.5 M NaCl	$P4_32_12$	*a* = 77.2 *b* = 77.2 *c* = 37.1	Chitin
Trypsin (PDB 5MNE)	23.3 kDa	Protein solution: 3 mM $CaCl_2$ with 10 mg/ml benzamidine Precipitant solution: 0.2 M $(NH_4)_2SO_4$ with 30% (w/v) PEG8000	$P2_12_12_1$	*a* = 54.7 *b* = 58.3 *c* = 66.9	Casein

Experimental

Reagents and equipment

All chemicals were at least 98% pure and solvents were pro-analysis grade. All produced magnetic supports were characterized by Fourier-transform infrared spectroscopy (FT-IR), dynamic light scattering (DLS), zeta potential and transmission electron microscopy (TEM). Infrared spectra were measured on a Tensor 27 FT-IR spectrometer from Bruker with dried MPs grounded and mixed with KBr (1:100). DLS and zeta potential (0.05 mg/ml solution in deionized water, pH 5.80, or other solution if otherwise stated) were measured on Dynamic Zetasizer NanoZS from Malvern instruments. TEM of magnetic particles samples were collected using Hitachi 8100 microscope operated with 200 kV of acceleration voltage with ThermoNoran light elements EDS detector and digital image acquisition.

Preparation of iron oxide magnetic particles

Fe_3O_4 magnetic particles (MP-Fe_3O_4) were prepared by the chemical co-precipitation method [20]. Briefly, 0.225 M $FeCl_3 \cdot 6H_2O$ (24.33 g in 400 ml of H_2O) and 1.43 M $FeCl_2 \cdot 4H_2O$ (10.79 g in 45 ml of H_2O) were mixed under mechanical stirring until homogenization was achieved. A 25% aqueous ammonia solution (75 ml) was added to the mixture under constant mechanical stirring (200 RPM). The resulting mixture was vigorously stirred for 5 minutes. MP-Fe_3O_4 were separated by a magnet and washed with distilled water (10 times) until pH 7 was reached.

A suspension of 10 mg/ml MP-Fe_3O_4 was sonicated for 15 minutes and further coated with a chitin (from shrimp shells) suspension (80 mg/ml; 20 mg in 2.5 ml), added dropwise to the MP-Fe_3O_4 suspension, under sonication. The mixture was incubated for 16 hours at 60°C with vigorous stirring (200 RPM). After this, the Fe_3O_4-chitin magnetic particles (MP-chitin) were separated by a magnet and washed (10 times) with distilled water. Chitin adsorption was measured by the anthrone method as previously described [21], with 90% adsorption achieved, yielding 7.2 mg chitin/mg MP-Fe_3O_4.

The synthesis of Fe_3O_4-casein magnetic particles (MP-casein), was adapted from Alves and co-authors protocol [22]. A solution of 10 ml of 0.225 M $FeCl_3 \cdot 6H_2O$ was added to 10 ml 1.43 M $FeCl_2 \cdot 4H_2O$ and next added to a 20 mg/ml casein (from bovine milk powder) solution in 100 mM Tris-HCl at pH 8.0. The mixture pH was adjusted to pH 11 using 25% ammonium hydroxide solution. Next, the mixture was incubated for 30 minutes at 50 °C under orbital shaking (200 RPM). MP-casein were separated by a magnet and washed with distilled water (10 times) until pH 7 was reached. The casein bound toFe_3O_4 magnetic core was quantified using absorption at 280nm, yielding 80% binding – 1.6 mg casein/mg MP-Fe_3O_4.

Static binding capacity

MP-Fe_3O_4 (0.5 mg/ml) and MP-chitin (0.5 mg/ml) in 0.5 M NaCl were separately incubated with HEWL at different concentrations (0.2 to 5 mg/ml) in 50 mM CH_3COONa at pH 4.5. MP-Fe_3O_4 (0.5 mg/ml) and MP-casein (0.5 mg/ml) in 0.2 M $(NH_4)_2SO_4$ with 30% (w/v) PEG8000 were separately incubated with trypsin at different concentrations (0.2 to 5 mg/ml) in (a) 3 mM $CaCl_2$ with 10 mg/ml benzamidine and (b) 3 mM $CaCl_2$. The interaction was promoted over 16 h at 20°C. The supernatants were collected, and fluorescence intensity was measured (λ_{ex} = 280 nm and λ_{em} = 340 nm). The adsorption phenomena followed a Hill isotherm (Equation 1) and the experimental data was fitted using OriginPro (v8.5.1).

$$q=\frac{\left(Q_{max} \times K_a \times C^{1-n}\right)}{1+K_a \times C^{1-n}} \qquad \text{Equation 1}$$

Where, q is the bound protein per mass of support (mg/g support) and C corresponds to the concentration of unbound protein in equilibrium (mg/ml).

Binding assay

HEWL (500 µl at 25 mg/ml) in 50 mM CH_3COONa at pH 4.5 was incubated with 500 µl of 0.5 mg/ml of MP-Fe_3O_4 and MP-chitin in 0.5 M NaCl for 1 hour at 20°C with 200 RPM orbital shaking. For trypsin, 500 µl of 60 mg/ml of trypsin in (a) 3 mM $CaCl_2$ with 10 mg/ml benzamidine and (b) 3 mM $CaCl_2$ were incubated with

500 µl of 0.5 mg/ml of MP-Fe_3O_4 and MP-casein in 0.2 M $(NH_4)_2SO_4$ with 30% (w/v) PEG8000, for 1 hour at 20°C with 200 RPM orbital shaking. The supernatants were collected, and fluorescence intensity was measured (λ_{ex} = 280 nm and λ_{em} = 340 nm). Iron leaching from MNPs under these conditions was negligible (below 5%) as previously shown [29].

Crystallization with magnetic particle additives

Crystallization assays were performed, as triplicates, using the hanging drop method in 24-well crystallization plates [30]. The crystallization setups were carried out at 20°C and drop inspections were performed using an optical microscope (V81 Stereo Microscope equipped with Camera – AxioCam Erc5s (5 MP), ZEISS). HEWL in 50 mM CH_3COONa at pH 4.5 (25 mg/ml) was crystallized using the following precipitant solutions: (i) 500 µl of 0.5 M NaCl, (ii) 0.5 mg/ml MP-Fe_3O_4 in 500 µl of 0.5 M NaCl and (iii) 0.5 mg/ml MP-chitin in 500 µl of 0.5 M NaCl, in 4 µl crystallization drops with 1:1 (v/v) protein-to-precipitant ratio. 60 mg/ml of trypsin from bovine pancreas in (a) 3 mM $CaCl_2$ with 10 mg/ml benzamidine and (b) 3 mM $CaCl_2$ were crystallized using the following precipitant solutions: (i) 500 µl of 0.2 M $(NH_4)_2SO_4$ with 30% (w/v) PEG8000, (ii) 0.5 mg/ml MP-Fe_3O_4 in 500 µl of 0.2 M $(NH_4)_2SO_4$ with 30% (w/v) PEG8000 and (iii) 0.5 mg/ml MP-casein in 500 µl of 0.2 M $(NH_4)_2SO_4$ with 30% (w/v) PEG8000, in 4 µl crystallization drops with 1:1 (v/v) protein-to-precipitant ratio. Prior to all assays with MPs, an MP suspension was added in the precipitant solution (to concentrations between 0.5-4 mg/ml of MPs in the precipitant solution), sonicated and homogenized for 10 minutes. After this, the desired volume was pipetted and mixed with the protein solution, following standard procedures [31–34].

Amount of protein crystallized

The crystallized proteins were harvested from the crystallization drops using a crystallization loop, washed in harvesting solution (with 10% more of the correspondent precipitant in solution) to avoid crystal solubilization and remove precipitated protein adsorbed to the crystal or MPs. Once cleaned, the crystals were solubilized in 10 mM phosphate buffer with 150 mM NaCl at pH 7.4 and centrifuged for 10 minutes at 2000 x*g* at room temperature. The supernatant was retrieved and compared with the loading sample in terms of amount of protein. HEWL and trypsin were quantified by λ_{ex} = 280 nm and λ_{em} = 340 nm.

X-ray diffraction and data processing

Data collections from all suitable protein crystals grown in the presence of different MP-Fe_3O_4 were carried out at the in-house X-ray diffraction facility using a Bruker D8 Venture Cu Kα X-ray generator coupled to a Photon 100 CMOS detector and an Oxford Cryo-Systems nitrogen stream at 100 K. All protein crystals were cryo-protected prior to flash-freezing in liquid nitrogen. HEWL and trypsin were cryo-protected using 20% glycerol added in the harvesting buffer. Data were indexed, integrated and scaled using PROTEUM3 software pipeline (Bruker AXS 2015) and converted to observed structure factors using SCALEPACK2MTZ and TRUNCATE from the CCP4 suite [35]. The structures were solved by molecular replacement using PhaserMR [36] within Phenix [37] with previously known structures of the proteins as search models (PDB 6F1L for HEWL and PDB 5MNE for trypsin). Electron density maps were generated and analysed with COOT [38]. The output model was further refined using PHENIX.REFINE [39]. Water molecules and solvent ions were also modelled into the structures, as indicated by mF_o-DF_c electron density maps.

Conclusions

This is the first report of a rationally-designed protein crystallization assay based on the addition of magnetic particles (MPs), coated or functionalized with affinity molecules towards a protein of interest, with the purpose of producing single crystals for 3D structure determination. Here, two different proteins were used to exemplify the straightforward approach offered by magnetic affinity crystallization. A high impact result is the MPs' potential as nucleation agents for the crystallization of enzymes hard to crystalize without its inhibitors, as demonstrated for trypsin crystallization using MP-casein as nucleation agent. The assays and results described in this proof-of-concept study are based on a single method of protein crystallization. Although vapor diffusion is currently the most employed protein crystallization method, it is of interest to evaluate the effect of MPs with other methods, namely batch or free interface diffusion.

HEWL is an extensively used protein in the search for innovative crystallization methods, and here also elected to investigate the influence of MPs as additives in protein crystallization. However, more than demonstrating the feasibility of using MPs and still be able to obtain protein crystals that diffract as optimally as the ones grown without the additives, we could witness faster onset of crystals with more protein (in mass) crystallized. This was particularly notorious when using affinity-triggered magnetic crystallization with MP-chitin.

Similarly to HEWL, bovine trypsin is also broadly used in crystallization studies as model protein. Nonetheless, as a protease, it is necessary to add benzamidine as an inhibitor of its proteolytic activity. Once added to the crystallization conditions, this inhibitor led to the decrease in the amount of protein bound to both MPs and to the decrease of K_a for the same MP. The depletion of benzamidine from the crystallization assays led to protein precipitation when no MP and MP-Fe_3O_4 was used as additive. However, when MP-casein was added, in 2 out of 3 crystallization drops, it was possible to achieve protein crystal growth without the need for benzamidine. Moreover, the addition of MPs led to a great increase in mass of crystallized protein, compared to the absence of MP additives, even in the presence of benzamidine.

Overall, the addition of MPs to the crystallization assays led to faster onset and growth of crystals. Affinity-triggered magnetic crystallization, a new example of heterogeneous nucleation [7], not only reduced the crystallization time, but also enabled the removal of critical additives as benzamidine, a trypsin inhibitor, usually necessary to obtain reproducible single crystals of

trypsin, as here described for the first time using affinity-coated MPs for enzyme crystallization without it's inhibitor. In all the tested proteins, MP addition did not notably change the crystal diffraction quality and unit cell parameters. Moreover, this work once again reinforces the versatility of MP coating and functionalization, here coated with a polysaccharide (chitin) and a protein (casein). Furthermore, the use of affinity driven MPs, such as MP-casein to crystallize trypsin, allowed to exclude the protease inhibitor, enabling the possible screening of different inhibitors or competition assays. Faster nucleation, seen in the crystallization of HEWL with chitin-coated MPs, and removal of undesired compounds, as seen in the crystallization of trypsin with casein-coated MPs, present as clear advantages, supporting the use of coated MPs in the attempts to address these specific problems in protein crystallization. The mechanism through which coated MPs influence and trigger nucleation and protein crystal growth should be investigated and will be the focus of future works.

Conflicts of interest

There are no conflicts to declare.

Acknowledgements

R. dos Santos acknowledges Fundação para a Ciência e Tecnologia (FCT-MCTES) - Portugal for the award of research fellowship PD/BD/105753/2014 and project grant RECI/BBB-BEP/0124/2012 (for usage of the in-house X-ray diffractometer). This work was supported by the Applied Molecular Biosciences Unit-UCIBIO, which is financed by national funds from FCT/MCTES (UIDB/04378/2020) and co-financed by the ERDF under the PT2020 Partnership Agreement (POCI-01-0145-FEDER-007728). R. dos Santos would like to recognize Dr. Ana Pina and Sara Carvalho, both from the Biomolecular Engineering Lab, for the laboratory support during protein expression and purification.

Notes and references

1 J. D. Westbrook and S. K. Burley, *Structure*, 2019, **27**, 211–217.

2 A.-L. Noresson, O. Aurelius, C. T. Öberg, O. Engström, A. P. Sundin, M. Håkansson, O. Stenström, M. Akke, D. T. Logan, H. Leffler and U. J. Nilsson, *Chem. Sci.*, 2018, **9**, 1014–1021.

3 J. F. Darby, M. Atobe, J. D. Firth, P. Bond, G. J. Davies, P. O'Brien and R. E. Hubbard, *Chem. Sci.*, 2017, **8**, 7772–7779.

4 C. Kotlowski, M. Larisika, P. M. Guerin, C. Kleber, T. Kröber, R. Mastrogiacomo, C. Nowak, P. Pelosi, S. Schütz, A. Schwaighofer and W. Knoll, *Sensors Actuators B Chem.*, 2018, **256**, 564–572.

5 G. Houlihan, P. Gatti-Lafranconi, D. Lowe and F. Hollfelder, *Protein Eng. Des. Sel.*, 2015, **28**, 269–79.

6 R. Li, V. Dows, D. J. Stewart, S. J. Burton and C. R. Lowe, *Nat. Biotechnol.*, 1998, **16**, 190–195.

7 R. P. Sear, *CrystEngComm*, 2014, **16**, 6506–6522.

8 C. Sauter, J. D. Ng, B. Lorber, G. Keith, Philippe Brion, M. Wais Hosseini, J.-M. Lehn and R. Giegé, *J. Cryst. Growth*, 1999, **196**, 365–376.

9 E. Girard, S. Olivier Maury, S. Engilberge, F. RiobéRiob, S. Di Pietro, L. Lassalle, N. Coquelle, C.-A. Arnaud, D. Pitrat, J.-C. Mulatier, D. Madern, E. Breyton and O. Maury, *Chem. Sci.*, 2017, **8**, 5909–5917.

10 B. Zhang, A. R. Mei, M. A. Isbell, D. Wang, Y. Wang, S. F. Tan, X. L. Teo, L. Xu, Z. Yang and J. Y. Y. Heng, *ACS Appl. Mater. Interfaces*, 2018, **10**, 44240–44246.

11 X.-Z. Yang, C.-Y. Zhang, Q.-J. Wang, Y.-Z. Guo, C. Dong, E.-K. Yan, W.-J. Liu, X.-W. Zheng and D.-C. Yin, *Cryst. Growth Des.*, 2017, **17**, 6189–6200.

12 D. Ribeiro, A. Kulakova, P. Quaresma, E. Pereira, C. Bonifácio, M. J. Romão, R. Franco and A. L. Carvalho, *Cryst. Growth Des.*, 2014, **14**, 222–227.

13 P. Asanithi, E. Saridakis, L. Govada, I. Jurewicz, E. W. Brunner, R. Ponnusamy, J. A. S. Cleaver, A. B. Dalton, N. E. Chayen and R. P. Sear, *ACS Appl. Mater. Interfaces*, 2009, **1**, 1203–1210.

14 Y. W. Chen, C. H. Lee, Y. L. Wang, T. L. Li and H. C. Chang, *Langmuir*, 2017, **33**, 6521–6527.

15 S. Khurshid, E. Saridakis, L. Govada and N. E. Chayen, *Nat. Protoc.*, 2014, **9**, 1621–1633.

16 S. Ko, H. Y. Kim, I. Choi and J. Choe, *Cryst. Growth Des.*, 2017, **17**, 497–503.

17 N. E. Chayen, E. Saridakis, R. El-Bahar and Y. Nemirovsky, *J. Mol. Biol.*, 2001, **312**, 591–595.

18 S. D. F. Santana, V. L. Dhadge and A. C. A. Roque, *ACS Appl. Mater. Interfaces*, 2012, **4**, 5907–5914.

19 L. Borlido, L. Moura, A. M. Azevedo, A. C. A. Roque, M. R. Aires-Barros and J. P. S. Farinha, *Biotechnol. J.*, 2013, **8**, 709–17.

20 L. Borlido, A. M. Azevedo, A. C. A. Roque and M. R. Aires-Barros, *J. Chromatogr. A*, 2011, **1218**, 7821–7827.

21 J. Skujins, A. Pukite and A. D. Mclaren, *Mol. Cell. Biochem.*, 1973, **2**, 221–228.

22 M. H. M. E. Alves, G. A. Nascimento, M. P. Cabrera, S. I. da C. Silvério, C. Nobre, J. A. Teixeira and L. B. de Carvalho, *Food Chem.*, 2017, **226**, 75–78.

23 U. V. Shah, D. R. Williams and J. Y. Y. Heng, *Cryst. Growth Des.*, 2012, **12**, 1362–1369.

24 M. Maeki, S. Ito, R. Takeda, G. Ueno, A. Ishida, H. Tani, M. Yamamoto and M. Tokeshi, *Chem. Sci.*, 2020, **11**, 9072–9087.

25 E. Rühmann, M. Betz, A. Heine and G. Klebe, *J. Med. Chem.*, 2015, **58**, 6960—6971.

26 J. Tang, C. L. Yu, S. R. Williams, E. Springman, D. Jeffery, P. A. Sprengeler, A. Estevez, J. Sampang, W. Shrader, J. Spencer, W. Young, M. McGrath and B. A. Katz, *J. Biol. Chem.*, 2005, **280**, 41077—41089.

27 J. Schiebel, R. Gaspari, T. Wulsdorf, K. Ngo, C. Sohn, T. E. Schrader, A. Cavalli, A. Ostermann, A. Heine and G. Klebe, *Nat. Commun.*, 2018, **9**, 3559.

28 M. Plaza-Garrido, M. C. Salinas-Garcia and A. Camara-Artigas, *Acta Crystallogr. Sect. D Struct. Biol.*, 2018, **74**, 480–489.

29 T. Barroso, T. Casimiro, A. M. Ferraria, F. Mattioli, A. Aguiar-Ricardo and A. C. A. Roque, *Adv. Funct. Mater.*, 2014, **24**, 4528–4541.

30 Y. R. Liang, L. N. Zhu, J. Gao, H. X. Zhao, Y. Zhu, S. Ye and Q. Fang, *ACS Appl. Mater. Interfaces*, 2017, **9**, 11837–11845.

31 R. dos Santos, C. S. M. Fernandes, S. Ottengy, A. C. Viecinski, G. Béhar, B. Mouratou, F. Pecorari and A. C. A. Roque, *J. Chromatogr. A*, , DOI:10.1016/j.chroma.2016.06.020.

32 I. L. Batalha, A. Hussain and A. C. A. Roque, *J. Mol. Recognit.*, 2010, **23**, 462–471.

33 A. C. A. Roque, A. Bicho, I. L. Batalha, A. S. Cardoso and A. Hussain, *J. Biotechnol.*, 2009, **144**, 313–320.

34 A. D'Arcy, A. Mac Sweeney and A. Haber, *Acta Crystallogr. - Sect. D Biol. Crystallogr.*, 2003, **59**, 1343–1346.

35 M. D. Winn, C. C. Ballard, K. D. Cowtan, E. J. Dodson, P. Emsley, P. R. Evans, R. M. Keegan, E. B. Krissinel, A. G. W. Leslie, A. McCoy, S. J. McNicholas, G. N. Murshudov, N. S. Pannu, E. A. Potterton, H. R. Powell, R. J. Read, A. Vagin and K. S. Wilson, *Acta Crystallogr. Sect. D Biol. Crystallogr.*, 2011, **67**, 235–242.

36 A. J. McCoy, R. W. Grosse-Kunstleve, P. D. Adams, M. D. Winn, L. C. Storoni and R. J. Read, *J. Appl. Crystallogr.*, 2007, **40**, 658–674.

37 P. D. Adams, P. V. Afonine, G. Bunkóczi, V. B. Chen, I. W. Davis, N. Echols, J. J. Headd, L.-W. Hung, G. J. Kapral, R. W. Grosse-Kunstleve, A. J. McCoy, N. W. Moriarty, R. Oeffner, R. J. Read, D. C. Richardson, J. S. Richardson, T. C. Terwilliger, P. H. Zwart and IUCr, *Acta Crystallogr. Sect. D Biol. Crystallogr.*, 2010, **66**, 213–221.

38 P. Emsley, B. Lohkamp, W. G. Scott and K. Cowtan, *Acta Crystallogr. Sect. D Biol. Crystallogr.*, 2010, **66**, 486–501.

39 P. V. Afonine, R. W. Grosse-Kunstleve, N. Echols, J. J. Headd, N. W. Moriarty, M. Mustyakimov, T. C. Terwilliger, A. Urzhumtsev, P. H. Zwart and P. D. Adams, *Acta Crystallogr. Sect. D Biol. Crystallogr.*, 2012, **68**, 352–367.